2004

Experimental Heat Transfer Coefficients and Pressure Drop During Refrigerant Vaporisation Inside Plate Heat Exchangers

Giovanni A. Longo
University of Padova

Andrea Gasparella
University of Padova

Roberto Sartori
Onda spa

EXPERIMENTAL HEAT TRANSFER COEFFICIENTS AND PRESSURE DROP DURING REFRIGERANT VAPORISATION INSIDE PLATE HEAT EXCHANGERS

Giovanni A. LONGO[1], Andrea GASPARELLA[1], Roberto SARTORI[2]

[1] University of Padova, Department of Management and Engineering
Stradella S. Nicola 3, I-36100 Vicenza - ITALY
Phone: +39 0444 998726 Fax: +39 0444 998888 E-Mail: tony@gest.unipd.it

[2] Onda S.p.A.
Via Baden Powel 11, I-36045 Lonigo (VI) – ITALY
Phone: +39 0444 720720 Fax: +39 0444 720721 E-Mail: ONDA@onda-it.com

ABSTRACT

This paper presents the experimental heat transfer coefficients and pressure drop measured during refrigerant vaporisation inside plate heat exchangers (PHE). Two different plates were tested: both present the same macro-scale herringbone corrugation, whereas they have different surface roughness. The smooth plate has an arithmetic mean roughness R_a of 0.4 μm, whereas the roughened plate presents a roughness R_a of 3.6 μm.
The prototypes were evaluated in vaporisation tests with refrigerant 22: a set of 34 experimental data was reported. The roughened plate shows an increase in the heat transfer coefficient around 30-40% with a penalty in friction losses around 25-30% with respect to the smooth plate.
Present experimental heat transfer coefficients were compared against semi-empirical correlations for pool-boiling: a fair agreement was found with Cooper (1984) and Gorenflo (1993) equations both for smooth and roughened plates.

1. INTRODUCTION

Plate heat exchangers (PHE) are commonly used for single-phase heat transfer from liquid to liquid having extensive application in the pharmaceutical industry, chemical processing and food treatment. In the last twenty years they are also used for two-phase heat transfer, particularly as evaporators and condensers in chillers and heat pumps. The application to high pressure refrigerant fluids required the development of a new type of PHE, the brazed plate heat exchangers (BPHE), in which the different plates are brazed and not linked by gaskets.
In open literature, it is possible to find several works on traditional PHE in single phase applications, whereas works on BPHE in refrigeration application are relatively scarce. Tonon et al. (1995) and Palm and Tonon (1999) presented good literature reviews on the thermal and hydraulic performances of plate heat exchangers in refrigerant condensation and vaporisation. More recently Yan & Lin (1999) experimentally investigated the effects of the mean vapour quality, mass flux, heat flux and pressure on heat transfer and pressure drop during vaporisation of refrigerant R134a inside a plate heat exchanger. They presented also empirical correlations for heat transfer coefficient and friction factor based on their experimental data. Hsieh and Lin (2002) reported experimental data on boiling heat transfer and pressure drop of refrigerant R410A in a plate heat exchanger. The effects of mass flux, heat flux, average vapour quality and pressure were evaluated and empirical correlations were proposed for heat transfer coefficient and friction factor. The experimental works on refrigerant vaporisation inside PHE by Engelhorn and Reihart (1990), Dutto et al. (1991), Claeson and Palm (1999) show that nucleate boiling is the dominant heat transfer regime. This regime is greatly affected by the surface roughness, which increases the nucleation site density.

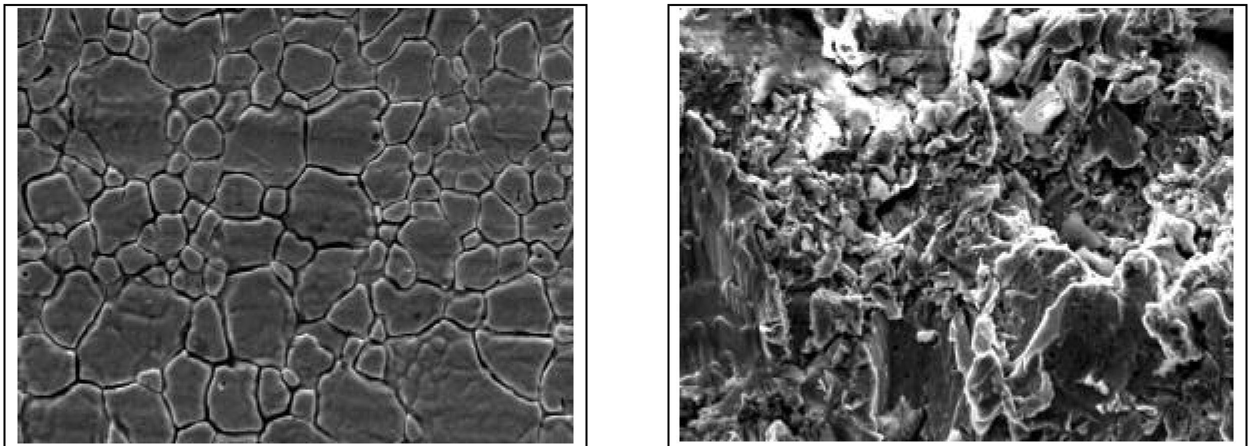

Smooth plate | Roughened plate

Figure 2: Smooth and roughened surface at the scanning electron microscope (1200 x)

The present work investigates the effect of an increase in the surface roughness of the plate on heat transfer and pressure drop during complete vaporisation of refrigerant 22 inside PHE. The experimental heat transfer coefficients are compared against semi-empirical correlations.

2. EXPERIMENTAL SET-UP

Two different prototypes have been realised: the reference prototype with smooth surface and the roughened prototype. Both the prototypes present the same macro-scale herringbone corrugation with an inclination angle of 65°, a corrugation amplitude of 2 mm, a corrugation pitch of 8 mm, whereas they have different surface roughness. The arithmetic mean roughness R_a, as defined in ISO 4271/1, of the reference smooth prototype is 0.4 µm, whereas the roughened prototype presents a roughness R_a of 3.6 µm. Figure 1 shows the comparison between the smooth and the roughened surface at the scanning electron microscope (1200 x): the roughened surface presents numerous cavities providing more and larger sites for bubble growth than the smooth surface. Each prototype consists of 4 plates and presents two channels on the water side (external channels) and a single channel on the refrigerant side (internal channel) to prevent an uneven distribution of the refrigerant between the channels. Figure 2 and table 1 give the main geometrical characteristics of all the different prototypes.

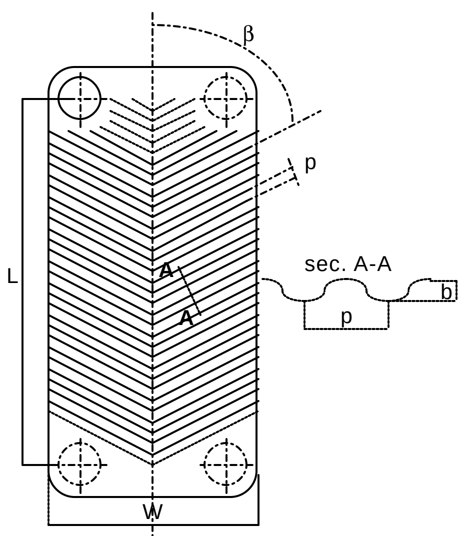

Figure 2: Schematic view of the plate

Table 1: Geometrical characteristics of the prototypes

Fluid flow plate length L(mm)	290
Plate width W(mm)	75
Nominal area of the plate A(m^2)	0.02175
Corrugation type	Herringbone
Angle of the corrugation β(°)	65
Corrugation amplitude b(mm)	2
Corrugation pitch p(mm)	8
Number of plates	4
Channels on refrigerant side	1
Channels on water side	2
Reference prototype roughness (µm)	0.4
Roughened prototype roughness (µm)	3.6

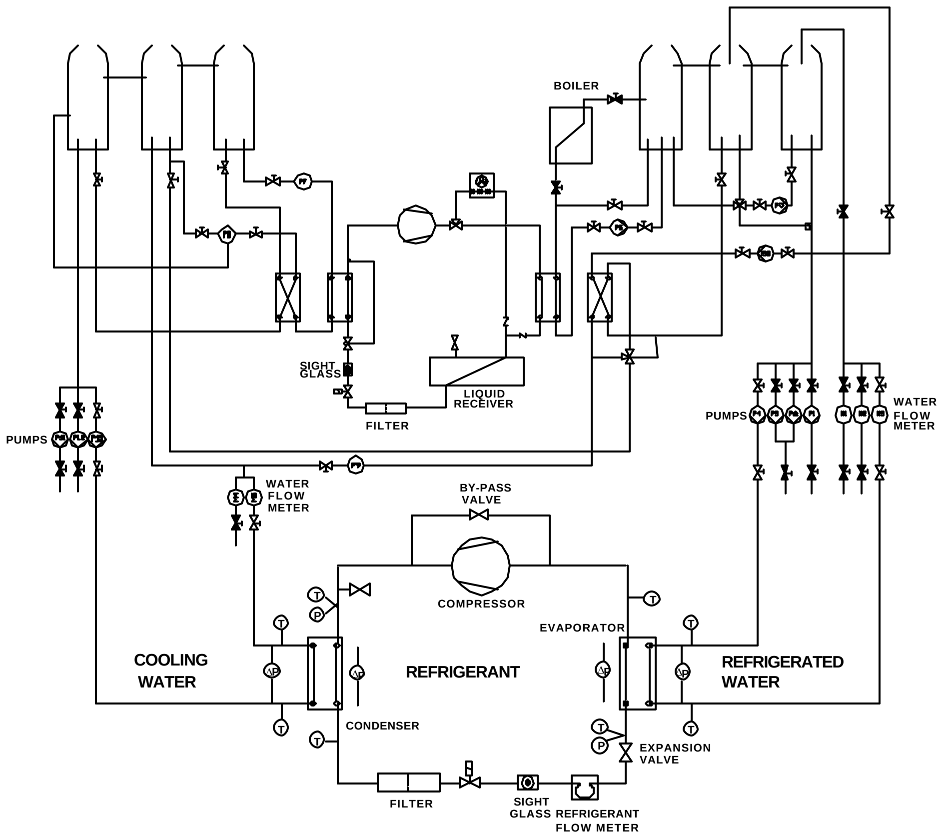

Figure 3: Schematic view of the experimental test rig

The above prototypes have been evaluated in an experimental rig for the measurement of the heat transfer coefficient and pressure drop during refrigerant vaporisation and condensation. The experimental facility, shown in figure 3, consists of a refrigerant loop, a cooling water loop and a refrigerated water loop. The first loop is a traditional chiller with a hermetic compressor and a manual throttling valve in which the condenser and the evaporator, supplied respectively with the cooling water and the refrigerated water, can be tested. The refrigerant mass flow rate is controlled by the throttling valve and by a by-pass valve of the hot-gas compressor. The refrigerant loop has no lubricant oil separator in order to reproduce the real operating conditions inside a vapour compression chiller in which the refrigerant flow is contaminated by lubricant oil in a variable percentage from 1 to 3%. The refrigerated water loop is able to supply a water flow at a temperature variable from 3 to 15°C with a stability within ±0.1 K, whereas the cooling water loop is able to supply a water flow at a temperature variable from 15 to 35°C with a stability within ±0.1 K. The refrigerant temperatures at the inlet and outlet of the condenser and the evaporator are measured by platinum resistance thermometers Pt100 having an accuracy of ±0.1 K. The refrigerant pressures at the inlet of the condenser and the evaporator are measured by strain-gage pressure transducers, having an accuracy of 0.075% f.s., whereas the pressure drops through evaporator and condenser are measured by strain-gage differential pressure transducers having an accuracy of 0.075% f.s.. The refrigerant mass flow rate is measured by means of a Coriolis effect mass flow meter having an accuracy of 0.1% of the measured value. The absolute atmospheric pressure is measured by a barometer having an accuracy of 0.08% f.s.. The refrigerated water and the cooling water mass flow rates are measured by means of a Coriolis effect mass flow meter having an accuracy of 0.1% of the measured value. The temperatures of the cooling water and the refrigerated water at the inlet and the outlet of the condenser and the evaporator respectively are measured by platinum resistance thermometers Pt100 having an accuracy of ±0.1 K. The pressure drop on the water side of the condenser and the evaporator are measured by strain-gage differential pressure transducers having an accuracy of 0.075% f.s.. All the measurements are scanned and recorded by a data logger linked to a P.C. Table 2 gives the main features of the different measuring devices in the experimental rig.

Table 2: Specification of the different measuring devices

Devices	**Type**	**Accuracy**	**Range**
Thermometers	- Pt100	0.1°K	-100 ÷ 500°C
Refrigerant flow meters	- Coriolis effect mass flow meter	0.1%	0 ÷ 180 kg/h
Water flow meters	- Coriolis effect mass flow meter	0.1%	0 ÷ 360 kg/h
Refrigerant pressure transducers	- Strain-gage	0.075% f.s.	0 ÷ 2.0 MPa
Differential pressure transducers	- Strain-gage	0.075% f.s.	0 ÷ 186 kPa
Barometer	- Strain-gage	0.080% f.s.	80 ÷ 120 kPa

3. DATA REDUCTION

3.1 Heat Transfer

The overall heat transfer coefficient U is equal to the ratio between the heat flow rate exchanged Q and the nominal heat transfer area S and the logarithmic mean temperature difference ΔT_{ln}.

$$U = Q / (S \Delta T_{ln}) \tag{1}$$

The heat flow rate exchanged is derived from a thermal balance on the water side:

$$Q = m_w c_{pw} \Delta T_w \tag{2}$$

where m_w is the water mass flow rate measured by the Coriolis mass flow meter, c_{pw} is the water specific heat capacity and ΔT_w is the temperature variation on the water side derived from the temperature measurements. The thermal balance on the water side is compared with the thermal balance on the refrigerant side:

$$Q_r = m_r \Delta J_r \tag{3}$$

where m_r is the refrigerant mass flow rate measured by the Coriolis mass flow meter and ΔJ_r is the enthalpy variation on the refrigerant side derived from the temperature and pressure measurements. Each test is acceptable only if the difference between the thermal balance on the water side and the refrigerant side is less than 3%.

The nominal heat transfer area

$$S = N A \tag{4}$$

is equal to the nominal projected area $A = L \times W$ of the single plate multiplied by the number N of the effective elements in heat transfer, as suggested by Shah and Focke (1988).

The logarithmic mean temperature difference is equal to

$$\Delta T_{ln} = [(T_{wo} - T_{wi}) / \ln [(T_s - T_{wo})/(T_s - T_{wi})] \tag{5}$$

where T_s is the saturation temperature of the refrigerant derived from the average pressure measured on refrigerant side, T_{wi} and T_{wo} the water temperatures at the inlet and the outlet of the heat exchanger measured by the platinum resistance thermometers Pt100. The logarithmic mean temperature difference is computed with reference to the saturation temperature on the refrigerant side neglecting any sub-cooling or superheating on refrigerant side as is usual in the design procedure. This assumption does not affect the results of the comparison between the different surfaces, as all the tests were carried out under the same superheating and sub-cooling.

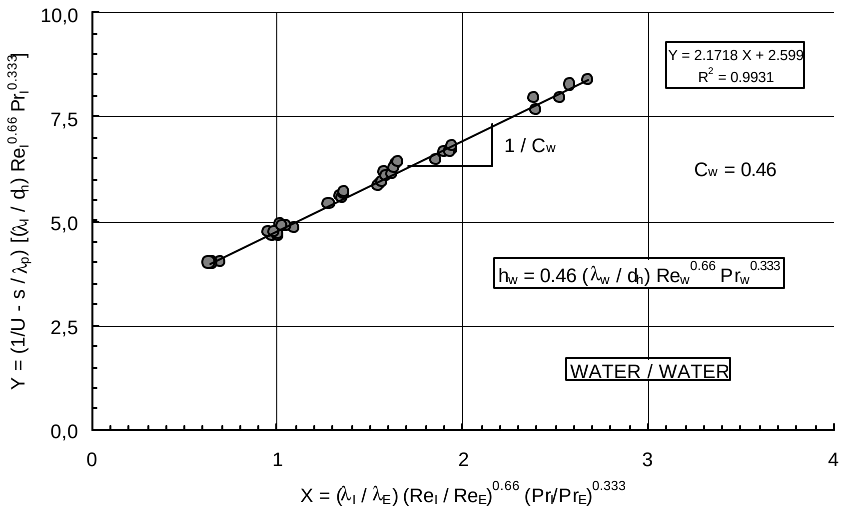

Figure 4: Modified Wilson plot results for calibration of water side heat transfer coefficient.

The heat transfer coefficients on the refrigerant side h_r were derived from the global heat transfer coefficient U:

$$h_r = (1 / U - s / \lambda_p - 1 / h_w)^{-1} \qquad (6)$$

by computing the water side heat transfer coefficient h_w using a modified Wilson plot technique. A specific set of experimental data consisting of more than 40 water to water data points was carried out on the prototype with smooth surface to determine the calibration correlation for heat transfer on the water side, in accordance with Muley & Manglick (1999). This modification of the classical Wilson plot technique incorporates an account of variable fluid property effects: figure 4 shows the water to water data plotted on the co-ordinates

$$X = (\lambda_I / \lambda_E)\,(Re_I / Re_E)^{0.66}\,(Pr_I/Pr_E)^{0.333} \qquad (7)$$

$$Y = (1/U - s / \lambda_p)\,[(\lambda_I / d_h)\,Re_I^{0.66}\,Pr_I^{0.333}] \qquad (8)$$

where subscripts I and E refer to the internal channel and to the external channels of the prototype tested.
The slope of the plot gives the constant in the calibration correlation, a power-law type, for heat transfer coefficients on the water side. The exponent on Reynolds number n = 0.66 was derived by a best fitting procedure on the experimental data. The calibration correlation for water side heat transfer coefficient results:

$$h_w = 0.46\,(\lambda_w / d_h)\,Re_w^{0.66}\,Pr_w^{0.333} \qquad (9)$$

$$350 < Re_w < 1100 \quad 5 < Pr_w < 10$$

It has to be noted that eq.(9) is only a calibration equation for the present test facility, valid only over the limited range of present water to water data. The refrigerant properties are evaluated by Refprop 6.1 (Nist 2001).
A detailed error analysis performed in accordance with Kline and McClintock (1953) indicates an overall accuracy within 12% for the refrigerant heat transfer coefficient measurement.

3.2 Pressure drop.

The frictional pressure drop ΔP_f was computed by subtracting the momentum pressure drop ΔP_a, the gravity pressure drop ΔP_g and the manifolds and ports pressure drops ΔP_c from the total pressure drop measured ΔP_t:

$$\Delta P_f = \Delta P_t - \Delta P_a - \Delta P_g - \Delta P_c \tag{10}$$

The momentum and gravity pressure drops were estimated by the homogeneous model for two-phase flow in the following form:

$$\Delta P_a = G^2 v_{fg} \Delta X \tag{11}$$

$$\Delta P_g = g\, L / v_m \tag{12}$$

where v_{fg} is the difference in specific volume between liquid and vapour phase, whereas v_m is the specific volume of the vapour-liquid mixture in the homogeneous model.
The pressure drops in the inlet and outlet manifolds and ports was empirically estimated, in accordance with Shah and Focke (1988):

$$\Delta P_c = 1.5\, (u_m^{\,2} / 2v_m)_i \tag{13}$$

where u_m is the mean flow velocity at the inlet port.
The accuracy of total pressure drop measurement is within ±7%.

4. ANALYSIS OF THE RESULTS

In the 34 experimental tests upflow of boiling refrigerant 22 in the central channel receives heat from the downflow of refrigerated water in the two others channels. The water inlet temperature T_{wi} was set at 12°C with a temperature decrease on the water side of 5°C, whereas on the refrigerant side the inlet vapour quality X_i ranges from 0.16 to 0.21 with an outlet superheating ΔT_{sup} around 4 ÷ 5°C. Table 3 gives the main operating conditions under experimental tests: refrigerant saturation temperature T_s, water inlet T_{wi} and outlet T_{wo} temperatures, refrigerant superheating ΔT_{sup}, inlet vapour quality X_i, mass flux on refrigerant side G_r and water side G_w, heat flux Q/S.

4.1 Heat Transfer

Figure 5 shows the refrigerant heat transfer coefficients against refrigerant heat flux. The roughened surface heat transfer coefficients are from 30 to 40% higher than the smooth surface. The correlation between heat transfer coefficients and heat flux is well represented by a power-law function with an exponent from 0.5 (smooth surface) to 0.6 (roughened surface) which is typical for nucleate boiling which, probably, is the dominant heat transfer regime in present vaporisation tests.

Table 3. Operating conditions during experimental tests.

Test	**Runs**	**T_s (°C)**	**ΔT_{sup} (°C)**	**X_i**	**T_{wi} (°C)**	**T_{wo} (°C)**	**G_r (kg/m^{2}s)**	**G_w (kg/m^{2}s)**	**Q/S (kW/m^2)**
Smooth plates	17	1.3 – 2.6	4.0 – 5.0	0.18-0.21	12.0	7.0	25.5 - 36.3	98.6-141.0	14.3 – 20.4
Roughened plates	17	2.2 - 3.2	4.0 – 5.0	0.16-0.21	12.0	7.0	26.3 – 38.2	102.2-150.9	14.9 - 21.9

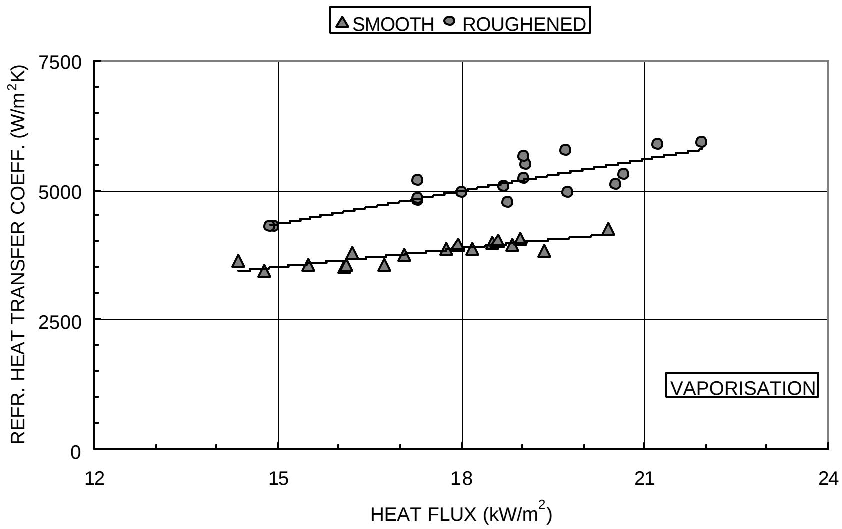

Figure 5: Heat transfer coefficients vs. heat flux under experimental tests.

The present experimental heat transfer coefficients were compared with Cooper (1984) and Gorenflo (1993) correlations. Cooper equation, developed for nucleate boiling, accounts for heat flux, surface roughness and reduced pressure effects. The Gorenflo equation is valid for pool boiling and accounts for heat flux, surface roughness and reduced pressure effects. Figure 6 shows the comparison between present experimental data and the above correlations: the mean absolute percentage deviation is around 5 and 7% for Gorenflo (1993) and Cooper (1984) respectively. This fair agreement seems to confirm that nucleate boiling controls present vaporisation data.

4.2 Pressure drop.

Figure 7 shows the frictional pressure drop during vaporisation tests against refrigerant Reynolds number: the roughened surface shows pressure drop 20% higher than the smooth surface. Therefore the roughened surface presents a penalty in pressure drop with respect to smooth surface lower than the enhancement in heat transfer.
In present experimental data the frictional pressure drop ranges from 93 to 96% of the total pressure drop and the maximum total pressure drop measured on refrigerant side, around 5 kPa, involves a very small saturation temperature decrease, around 0.3°C, with negligible effect on heat transfer.

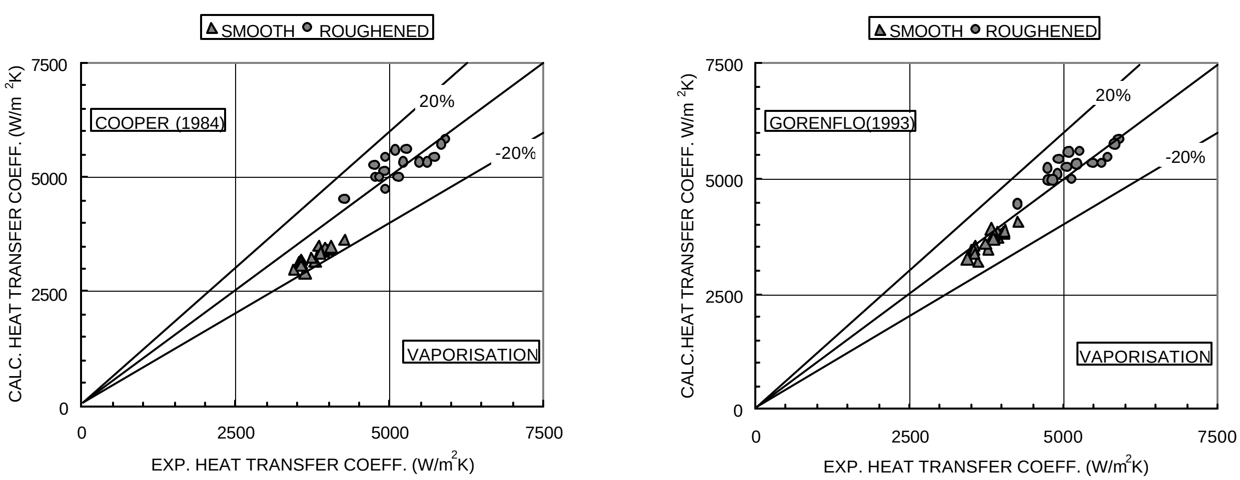

Figure 6: Comparison between experimental heat transfer coefficients and semi-empirical correlations.

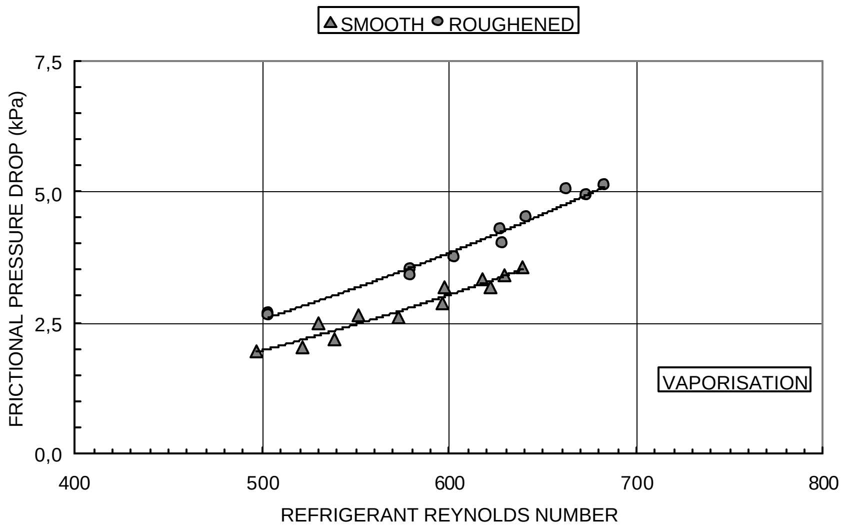

Figure 7: Frictional pressure drop vs. refrigerant Reynolds number under experimental tests.

5. CONCLUSION

This paper investigates the effect of an increase in the surface roughness of the plate on heat transfer and pressure drop during complete vaporisation of refrigerant 22 inside PHE: 34 experimental data points were reported.
The roughened surface shows a penalty in pressure drop with respects to the smooth surface around 20%, lower than the enhancement in heat transfer coefficients which ranges from 30 to 40%.
A fair agreement was found between present experimental heat transfer coefficients and the Gorenflo (1993) and Cooper (1984) semi-empirical correlations for pool boiling.

REFERENCES

Claeson, J., Palm, B., 1999, Boiling mechanism in a small compact brazed plate heat exchanger (CBE) by using thermochromic liquid crystals (TLC), *Proc. 20th Int. Congr. Refr*., Sydney, Australia, paper 1177

Cooper, M.G., 1984, Heat flows rates in saturated pool boiling – A wide ranging examination using reduced properties, *Advanced in Heat Transfer*, Academic Press, Orlando, Florida, p.157-239

Dutto, T., Blaise, J.C., Benedic, T., 1991, Performances of brazed plate heat exchanger set in heat pump, *Proc. 18th Int. Congr. Refr*., Montreal, Canada, p. 1284-1288.

Engelhorn, H.R., Reihart, A.M., 1990, Investigations on heat transfer in plate evaporators, *Chem. Eng. Process*, vol.28, p. 143-146.

Gorenflo, D., 1993, Pool boiling, *VDI Heat Atlas*, Dusseldorf, Germany, p. Ha1-25.

Hsieh, Y.Y., Lin, T.F., 2002, Saturated flow boiling heat transfer and pressure drop of refrigerant R410A in a vertical plate heat exchanger, *Int. J. of Heat and Mass Transfer*, vol. 45, p. 1033-1044.

Kline,S.J., McClintock,F.A.,1953, Describing uncertainties in single-sample experiments, *Mech.Eng*.,vol.75,p.3-8.

Muley, A., Manglik, R.M., 1999, Experimental study of turbulent flow heat transfer and pressure drop in a plate heat exchanger with chevron plates, *Asme J. of Heat Transfer*, vol.121, p.110-121.

NIST, 2001, Refrigerant properties computer code, REFPROP 6.1.

Palm, B., Thonon, B., 1999, Thermal and hydraulic performances of compact heat exchangers for refrigeration systems, *Proc. of Int. Conf. on Compact Heat Exchangers and Enhancement Technology for the Process Industries*, Banff, Canada, p. 455-462.

Shah, R.K., Focke, W.W., 1988, Plate heat exchangers and their design theory, *Heat Transfer Equipment Design*, Hemisphere, Washington, p. 227-254.

Thonon, B., Vidil, R., Marvillet, C., 1995, Recent research and developments in plate heat exchangers, *J. of Enhanced Heat Transfer*, vol.2, p. 149-155.

Yan, Y.Y., Lin, T.F., 1999, Evaporation heat transfer and pressure drop of refrigerant R-134a in a plate heat exchanger, *ASME J. of Heat Transfer*, vol.121, p. 118-127.